Journal of Luminescence 164 (2015) 112–115

Contents lists available at ScienceDirect

Journal of Luminescence

journal homepage: www.elsevier.com/locate/jlumin

Study of optically stimulated luminescence of Tb^{3+}/Sm^{3+} doubly doped K_2YF_5 single crystals

J. Marcazzó [a,*], L. Camargo [a], N.M. Khaidukov [b], M. Santiago [a]

[a] Instituto de Física Arroyo Seco – CIFICEN (CONICET–UNCPBA), Pinto 399, 7000 Tandil, Argentina
[b] Kurnakov Institute of General and Inorganic Chemistry, RAS, Leninskii Prospekt 31, 119991 Moscow, Russia

ARTICLE INFO

Article history:
Received 18 June 2014
Received in revised form
22 December 2014
Accepted 25 March 2015
Available online 2 April 2015

Keywords:
Optically stimulated luminescence
K_2YF_5 crystals
Terbium
Samarium

ABSTRACT

In this work the optically stimulated luminescence (OSL) properties of K_2YF_5 crystals doubly doped with Tb^{3+} and Sm^{3+} ions have been investigated for the first time. The OSL response of K_2YF_5 crystals containing different dopant concentrations under optical stimulation with different wavelengths has been analyzed. Dosimetric properties of the most efficient composition, namely, K_2YF_5:1.0 at% Tb^{3+};1.0 at% Sm^{3+}, have been studied. Finally, the possible application of this single crystal to OSL dosimetry has been evaluated.

1. Introduction

In the last years, optically stimulated luminescence (OSL) has become a better alternative for radiation dosimetry than thermally stimulated luminescence (TL) due to several advantages. In particular, readout process is faster in OSL as compared to TL due to the fact that optical instead of thermal stimulation is employed. Besides, OSL presents high sensitivity, simpler readers and easier automation. Since readout of OSL dosimeters do not require high temperature, OSL phosphors can be mixed with or embedded in plastic hosts in order to make sturdy dosimeters. For the same reason, no thermal quenching effects are observed during OSL readout. Finally, TL dosimetry is a destructive technique, i.e., readout requires heating of a detector and the signal is completely removed from the dosimeter. In the case of OSL dosimeters several readouts can be made in order to check the dose assessment [1].

Currently only a few materials that show promising properties to be applied in OSL dosimetry have been developed and commercially deployed. In particular, Al_2O_3:C and BeO ceramics are suitable for OSL dosimetry. Nevertheless, there is a permanent interest in searching for new OSL materials with improved dosimetric properties, namely, high OSL efficiency, high repeatability and reproducibility of the OSL signal, wide linear dose response range, minimal OSL fading, etc.

Several K_2YF_5 fluorides doped with optically active rare earth ions, in particular, Pr^{3+}, Tb^{3+} and Sm^{3+} show very efficient radiation-induced emission [2–5]. In fact, it has been found that K_2YF_5:Tb^{3+};Sm^{3+} shows thermoluminescence and radioluminescence properties, which are attractive for dosimetry purposes [5]. Recently, the OSL properties of K_2YF_5:Pr^{3+} and K_2YF_5:Tb^{3+} have been studied and it has been found that these doped fluorides show linear OSL response and repetitive dosimetric properties [6,7]. In the case of K_2YF_5:Tb^{3+} fading of the OSL signal has been observed, which is slightly higher than 40% after one day of storage of the irradiated sample at dark and at room temperature [7].

There is evidence that Sm^{3+} may play the role of deep electron trap when included as dopant in different hosts. In fact, Dorenbos and Bos reported that in TL experiments YPO_4:Sm,Ce electrons trapped in Sm^{3+} radiatively recombine with holes trapped in Ce^{3+} giving rise to Ce^{3+} characteristic emission [8]. Similar processes could be expected if Ce^{3+} is replaced by Tb^{3+} or Pr^{3+}. In this context, including Sm^{3+} cations as co-dopant might be useful to increase the concentration of traps thermally stable at room temperature.

The goal of this work is to study the OSL properties of K_2YF_5 single crystals doubly-doped with Tb^{3+} and Sm^{3+} with the aim of evaluating the feasibility of using these compounds as OSL dosimeters. In particular, the dose response, OSL spectrum, OSL efficiency after red and green light stimulation, OSL efficiency as a function of doping concentration and the fading of the OSL signal at room temperature of K_2YF_5:Tb^{3+},Sm^{3+} have been investigated.

2. Experimental

Crystals of orthorhombic K_2YF_5 fluoride doped with optically active rare earth ions were grown under hydrothermal conditions. For hydrothermal experiments, copper insert lined autoclaves having a volume of about 40 cm^3 were utilized and the inserts

* Corresponding author. Tel.: +54 249 438 5660.
E-mail address: jmarcass@exa.unicen.edu.ar (J. Marcazzó).

http://dx.doi.org/10.1016/j.jlumin.2015.03.031
0022-2313/

were separated into synthesis and crystallization zones by perforated diaphragms. The fluoride crystals were synthesized by a direct temperature-gradient method as a result of the reaction of the aqueous solutions containing 40–50 mol% KF with oxide mixtures $(1-x-y)$ Y_2O_3–xSm_2O_3–$yTb_2O_{3,5}$ at a temperature of about 750 K in the synthesis zone, a temperature gradient along the reactor body up to 3 K cm^{-1}, and a pressure of about 100 MPa. Under these conditions, spontaneously nucleated crystals up to 0.5 cm^3 in size were grown in the upper crystallization zone of the autoclave for 200 h [9]. The structure type and phase purity of synthesized samples were characterized by powder X-ray diffraction and the purities of the utilized oxides were 99.99% [10].

The crystals were irradiated at room temperature (RT) with a 3.7×10^8 Bq ophthalmic ^{90}Sr beta-source rendering a dose rate of 0.022 Gy min^{-1} at the sample position. For the optical stimulation, a Luxeon V Star green LED with maximum emission at 530 nm and a Luxeon III Star red LED with maximum emission at 627 nm were used. These LEDs were driven at 500 mA with a Laser Diode Driver model 525B of Newport. The effective luminous flux for the green and red LEDs at the sample position amounted to 128 and 56 lm respectively. Two 3 mm thick Schott OG530 long-pass filters were placed in front of the LEDs and two 3 mm thick Hoya B-390 band-pass filters were interposed between the sample and the light detector in order to prevent the stimulation light to reach the light detector. The Schott OG530 filter features a maximum transmission of 0.91 for wavelengths higher than 530 nm and a transmission less than 10^{-6} at shorter wavelengths. The B-390 has the maximum transmission at 400 nm and the transmission window is localized between 320 and 500 nm. The OSL signal was measured by using a Sens-Tech P25PC-02 photon counting photomultiplier tube (PMT) and all measurements were performed at RT.

Radioluminescence spectra were recorded by means of an Acton Research SP-2155 0.150 m monochromator featuring a Hamamatsu H9319 photon counting PMT having sensitivity between 300 and 850 nm. Spectra were measured within the wavelength range of 300–800 nm and at a rate of 20 nm min^{-1}. The sample was placed at the entrance slit and irradiated with the aforementioned beta-source, which was situated 1 cm away from the sample. A resolution of approximately 5 nm was obtained by setting the entrance and exit slits width at 3 mm during the measurements. OSL spectrum was measured by means of the same setup and using green light stimulation. The B-390 band pass filter was placed between the sample and the monochromator in order to cut off the stimulation light.

TL glow curves from the samples were recorded from RT up to 375 °C with a constant heating rate of 1.0 K s^{-1} by using a Harshaw–Bicron 3500 TL reader featuring a Hamamatsu R6094 photomultiplier tube.

3. Results and discussions

In order to maximize the collection of the light emitted by the stimulated sample and to determine the most suitable combination of optical filters to be employed for the OSL experiments, it is necessary to know the emission spectra of the compounds under study. In some cases, the spectrum of the light emitted during irradiation, namely, the RL spectrum, is similar to the OSL spectrum. For this reason it is worth recording both spectra in order to determine whether the optically active centers involved in both phenomena are the same.

In Fig. 1a and b the RL spectra of K_2YF_5:1.0 at% Tb^{3+};1.0 at% Sm^{3+} and K_2YF_5:1.0 at% Tb^{3+};0.5 at% Sm^{3+} are depicted respectively. Both RL spectra show several bands at 380, 415, 480, 550, 600, 650, 710 and 760 nm having different intensities. The first four bands can be attributed to characteristic 4f–4f Tb^{3+} transitions of Tb^{3+}, namely,

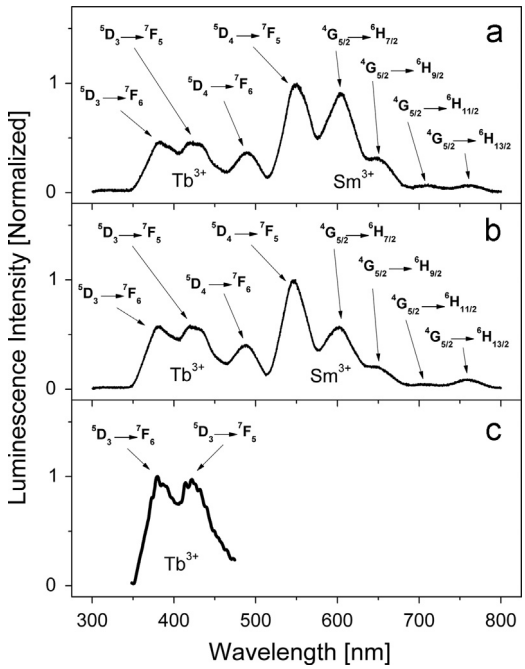

Fig. 1. RL spectra of K_2YF_5:1.0 at% Tb^{3+};1.0 at% Sm^{3+} (a) and K_2YF_5:1.0 at% Tb^{3+};0.5 at% Sm^{3+} (b). Curve (c) corresponds to the OSL spectrum of K_2YF_5:1.0 at% Tb^{3+};1.0 at% Sm^{3+}.

$^5D_3 \rightarrow {}^7F_j$ and $^5D_4 \rightarrow {}^7F_j$ with $j=6$ and 5 in each case respectively [5,11]. On the other hand, bands at 600, 650, 710 and 760 nm can be attributed to characteristic 4f–4f transitions in Sm^{3+}, namely, $^4G_{5/2} \rightarrow {}^6H_j$ with $j=7/2$, 9/2, 11/2 and 13/2 respectively [12,13]. Besides, the peak centered at 550 nm can be assigned to the overlap of the $^5D_4 \rightarrow {}^7F_5$ Tb^{3+} and the $^4G_{5/2} \rightarrow {}^6H_{5/2}$ transitions of Sm^{3+}. It is evident from Fig. 1a and b that the intensity ratios of the RL peaks depend on the concentration of Sm^{3+} ions co-doped in K_2YF_5:1.0 at% Tb^{3+}. As expected, the height of Sm^{3+} peaks increases relative to those of Tb^{3+} as the concentration of Sm goes up.

In Fig. 1c, the OSL spectrum of K_2YF_5:1.0 at% Tb^{3+};1.0 at% Sm^{3+} under green light stimulation is also depicted. It is apparent from Fig. 1c that the OSL emission bands at 380 and 420 nm correspond to transitions $^5D_3 \rightarrow {}^7F_6$ and $^5D_3 \rightarrow {}^7F_5$ of Tb^{3+} respectively. Because of the B-390 filter employed to record the OSL emission information about spectral components beyond 500 nm is missing. In particular, it is not possible to assess whether Sm^{3+} characteristic emission is present in the OSL spectrum beyond the filter cut-off wavelength.

Fig. 2 shows the effect of red and green stimulation on the OSL response of K_2YF_5:1.0 at% Tb^{3+};1.0 at% Sm^{3+} after irradiating the sample with a dose of 2 Gy. It is apparent from the figure that OSL signal is more intense when green light is employed. This result has been observed in all of the studied samples and also in previous works regarding the OSL of K_2YF_5:Pr^{3+} and K_2YF_5:Tb^{3+} [6,7]. By taking into account this result, all the OSL measurements throughout this work have been carried out by stimulating the samples with the green LED.

Fig. 3 shows the OSL response of the irradiated samples under green light stimulation as a function of time. From top to bottom the OSL decay curves correspond to K_2YF_5:1.0 at% Tb^{3+};1.0 at% Sm^{3+}, K_2YF_5:1.0 at% Tb^{3+};2.0 at% Sm^{3+} and K_2YF_5:1.0 at% Tb^{3+};0.5 at% Sm^{3+}, respectively. Each sample has been irradiated with a dose of 2 Gy and the OSL intensity has been normalized to the sample weight. It can be seen from the figure that the composition K_2YF_5:1.0 at% Tb^{3+};1.0 at% Sm^{3+} is the most efficient OSL phosphor. According to Dorenbos and Bos it is expected that during irradiation Sm^{3+} provides deep traps for electrons that later recombine at Tb sites during optically stimulated relaxation

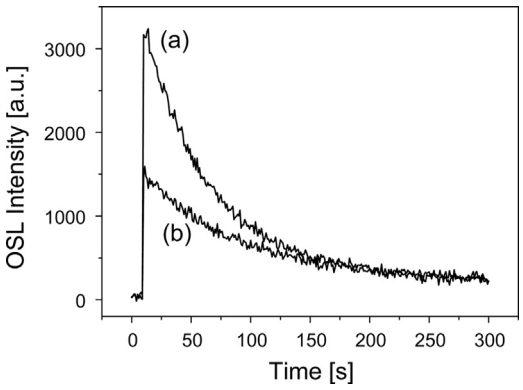

Fig. 2. OSL decay curves of K_2YF_5:1.0 at% Tb^{3+};1.0 at% Sm^{3+} under green (a) and red (b) light stimulation.

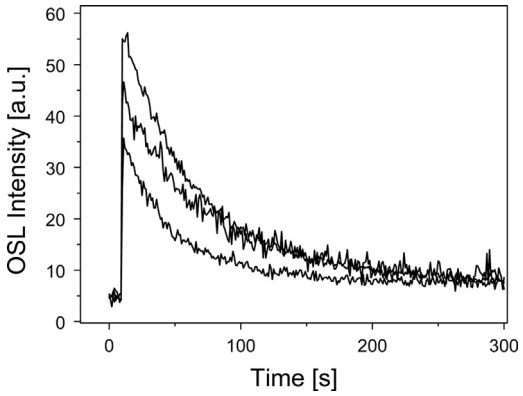

Fig. 3. OSL decay curves of irradiated K_2YF_5:1.0 at% Tb^{3+};1.0 at% Sm^{3+}, K_2YF_5:1.0 at% Tb^{3+};2.0 at% Sm^{3+} and K_2YF_5:1.0 at% Tb^{3+};0.5 at% Sm^{3+}, from top to bottom, respectively, under green light stimulation.

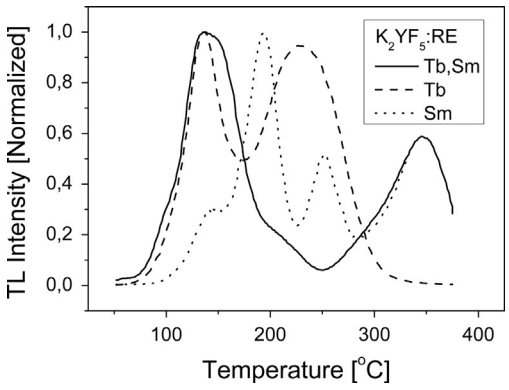

Fig. 4. TL glow curves of K_2YF_5:Tb^{3+},Sm^{3+} (solid), K_2YF_5:Tb^{3+} (dash) and K_2YF_5:Sm^{3+} (dot).

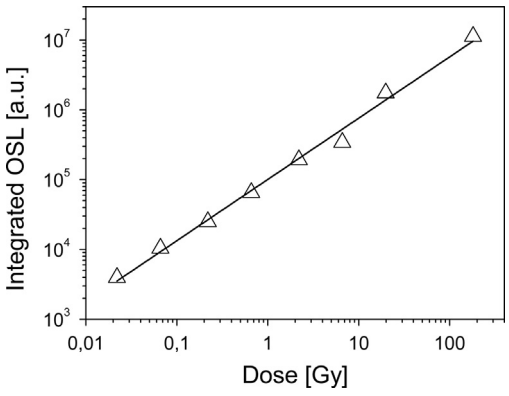

Fig. 5. OSL dose response of the integrated OSL signal for K_2YF_5:1.0 at% Tb^{3+};1.0 at% Sm^{3+} exposed to different beta doses (hollow triangles) under green light stimulation. Full line was obtained by linear regression and included for eye-guiding purposes.

[8]. In this context, the most intense OSL emission should be observed for the K_2YF_5:Tb^{3+},Sm^{3+} crystals being doped with the highest Sm concentration, namely, K_2YF_5:1.0 at% Tb^{3+};2.0 at% Sm^{3+}. However, this is not certainly the case. In principle it is possible that several kinds of Sm-related defects coexist in K_2YF_5, which could work not only as traps but also as recombination centers during the OSL process. This competing condition would easily lead to the observed result, say, an intermediate Sm concentration renders the maximum OSL emission. In fact, similar behavior has been reported in previous studies of the OSL of Pr^{3+} and Tb^{3+}-doped K_2YF_5 [6,7].

The complexity of the trap structure of K_2YF_5:Tb^{3+},Sm^{3+} is revealed by its glow curve as shown in Fig. 4 (solid line), where it is also compared with the glow curves of singly-doped K_2YF_5:Tb^{3+} (dash) and K_2YF_5:Sm^{3+} (dot) compounds. A rather complex structure made up of several overlapping peaks shows up in all of the three glow curves. It is apparent that the high temperature peak at 350 °C is due to the inclusion of Sm as dopant, since this peak does not appear at all in the glow curve of K_2YF_5:Tb^{3+}. Similarly, the intense peak band at low temperature, which is observed in the glow curve of K_2YF_5:Tb^{3+},Sm^{3+} and K_2YF_5:Tb^{3+}, might be assigned to the presence of Tb. The exact role played by Sm and Tb during the luminescence process could be determined by recording the TL spectrum as a function of the temperature. Besides, it is likely that some of the traps and recombination centers involved in TL also participate in the OSL process. However, a detailed study implying correlated TL/OSL experiments and glow curve deconvolution would be necessary to support the previous statement.

In order to evaluate the feasibility of using this material as OSL dosimeter, the dosimetric characteristics of the most efficient composition K_2YF_5:1.0 at% Tb^{3+};1.0 at% Sm^{3+} have been studied. Fig. 5 shows the OSL dose–response obtained within the range from 0.02 to 200 Gy. Good linearity and no saturation in the studied dose range is observed. Besides, the minimum detectable dose (MDD) of this composition has been determined by adopting the simple definition put forward by Yukihara and McKeever [14]. According to this definition MDD$=3\sigma_{BG}$, being σ_{BG} the experimental standard deviation of the background signal recorded by using blank detectors, namely, the same detectors as those used for the measurements, except that they are not irradiated. For K_2YF_5:1.0 at% Tb^{3+};1.0 at% Sm^{3+}, MDD has been found to be 0.02 Gy.

From the point of view of the application of this compound to OSL dosimetry, it is of interest to investigate the fading of the OSL signal as a function of the time elapsed between irradiation and readout. This fading is frequently related to the depopulation of shallow traps occupied by charges excited by ionizing radiation. In this context, the OSL signal of K_2YF_5:1.0 at% Tb^{3+};1.0 at% Sm^{3+} crystals irradiated with a dose of 2 Gy and kept in dark and at room temperature for different times has been measured. Fig. 6 shows the integrated OSL signal as a function of several storing times, namely, 0.05, 0.08, 0.16, 1.66, 16.66 and 168 h. It can be seen from the figure that the OSL signal shows a fading of approximately 33% after the first 24 h of storing and then, the response remains constant. This behavior is an evidence that at least two kinds of traps, namely, shallow and thermally stable traps, are responsible for OSL in K_2YF_5:Tb^{3+},Sm^{3+}. On the other hand, it is worth mentioning that the fading of the OSL signal of Tb–Sm-doubly doped K_2YF_5 is slightly lower (33%) than that of Tb-singly doped K_2YF_5 (40%) [7]. In principle, this more favorable behavior could be ascribed to the presence of Sm-related traps [8]. We have investigated whether similar fading

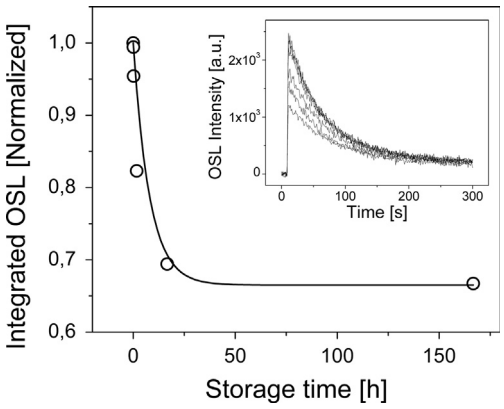

Fig. 6. Integrated OSL signal corresponding K_2YF_5:1.0 at% Tb^{3+};1.0 at% Sm^{3+} as a function of the storage time (hollow circles). Continuous line was obtained by fitting a single exponential decay and included for eye-guiding purposes. Inset: the OSL response after 0.05, 0.08, 0.16, 1.66, 16.66 and 168 h of storage, from top to bottom one after another.

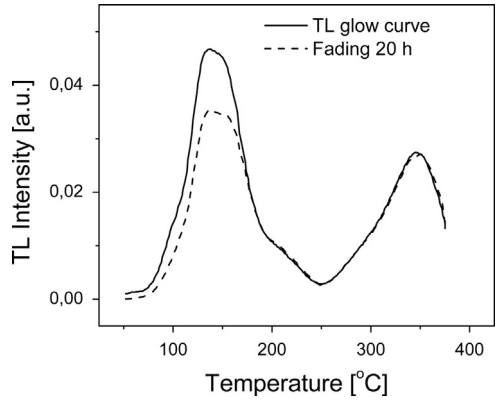

Fig. 7. Fading of the glow curve of K_2YF_5:1.0 at% Tb^{3+}; 1.0 at% Sm^{3+} measured 20 h after irradiation (dash). The glow curve as measured promptly after irradiation has been included for reference (solid).

effects are observed in the TL signal of this compound. In Fig. 7 the glow curve of K_2YF_5:1.0 at% Tb^{3+};1.0 at% Sm^{3+} crystals measured immediately after irradiation and after 20 h of storage in dark and at room temperature are shown. There is an evident decrease of the intensity of the peaks corresponding to the low temperature portion of the glow curve of K_2YF_5:Tb^{3+},Sm^{3+}. These results could be evidence that the thermally unstable traps responsible for the low temperature peaks could also participate in OSL process. In this case and for dosimetry purposes a short annealing around 120 °C performed just before the OSL readout would be enough to get rid of the fading component of the OSL signal of K_2YF_5:Tb^{3+},Sm^{3+} [7].

4. Conclusions

The OSL dosimetric properties of K_2YF_5:Tb^{3+},Sm^{3+} have been investigated for the first time. In particular, K_2YF_5:1.0 at% Tb^{3+};1.0 at% Sm^{3+} has been found to be the most efficient of the studied rare earth ion concentrations and this composition shows good linearity in the dose range of 0.02–200 Gy. Besides, a minimum detectable dose of 0.02 Gy and no saturation in the studied range have been found. Tb/Sm doubly doped K_2YF_5 provides a more stable OSL signal with respect to Tb-singly doped K_2YF_5.

Acknowledgments

We acknowledge the financial support received from PICT 2012-0715 (ANPCyT, Argentina) and PIP 1076 2012-2014 (CONICET, Argentina).

References

[1] M.S. Akselrod, L. Botter-Jensen, S.W.S. McKeever, Radiat. Meas. 41 (2007) S78.
[2] L.O. Faria, D. Lo, H.W. Kui, N.M. Khaidukov, M.S. Nogueira, Radiat. Prot. Dosim. 102 (2004) 435.
[3] J. Marcazzó, M. Santiago, E. Caselli, N. Nariyama, N.M. Khaidukov, Opt. Mater. 26 (2004) 65.
[4] J. Marcazzó, J. Henniger, N.M. Khaidukov, V.N. Makhov, E. Caselli, M. Santiago, J. Phys. D: Appl. Phys. 40 (2007) 5055.
[5] J. Marcazzó, M. Santiago, V.N. Makhov, Vu. Phi Tuyen, N.M. Khaidukov, E. Caselli, J. Lumin. 140 (2013) 82.
[6] J. Marcazzó, N.M. Khaidukov, E. Caselli, C. Dangelo, M. Santiago, Phys. Status Solidi A 206 (2009) 2593.
[7] J. Marcazzó, E. Cruz-Zaragoza, Vu Xuan Quang, N.M. Khaidukov, M. Santiago, J. Lumin. 131 (2011) 2711.
[8] P. Dorenbos, A.J.J. Bos, Radiat. Meas. 43 (2008) 139.
[9] M.A. Dubinskii, N.M. Khaidukov, I.G. Garipov, L.N. Dem'yanets, A.K. Naumov, V.V. Semashko, V.A. Malyusov, J. Mod. Opt. 37 (1990) 1355.
[10] N.M. Khaidukov, P.P. Fedorov, L.N. Dem'yanrts, I.P. Zibrov, V.A. Malyusov, Russ. J. Inorg. Chem. 35 (1990) 383.
[11] A.J. Bos, M. Prokic, J.C. Brouwer, Radiat. Prot. Dosim. 119 (2006) 130.
[12] A. Thulasiramudu, S. Buddhudu, Spectrochim. Acta A 67 (2007) 802.
[13] B.H. Rudramadevi, S. Buddhudu, Indian J. Pure Appl. Phys. 46 (2008) 825.
[14] E.G. Yukihara, S.W.S. McKeever, Optically Stimulated Luminescence: Fundamentals and Applications, John Wiley & Sons Ltd., The Atrium, Southerm Gate, Chischester, West Sussex, United Kingdom, 2011.